



ISSN 1110-0451

Web site: ajnsa.journals.ekb.eg



(E S N S A)

Investigation of production of neutral Higgs boson and two charged charginos from electron-positron annihilation via different propagators

Sara Abdelrady Hassan¹, Asmaa.A. A², Sherif Yehia³, M.M. Ahmed³ and Mohammed Said Mohammed Abu-Elmagd^{1*}

⁽¹⁾Department of Engineering Mathematics and Physics, Higher Institute of Engineering, El-Shorouk Academy, El-Shorouk City, Egypt

⁽²⁾Egyptian Organization for Standardization and Quality, Cairo, Egypt

⁽³⁾Department of Physics, Faculty of Science, Helwan University, Cairo, Egypt

ARTICLE INFO

Article history:

Received: 6th Feb. 2023

Accepted: 6th May 2023

Available online: 14th June 2023

Keywords:

Higgs boson,

Chargino and Neutralino.

ABSTRACT

In the current work, the production of neutral Higgs boson (H_ℓ^0) and two charged Charginos ($\tilde{\chi}_i^+, \tilde{\chi}_j^-$) owing to electron-positron annihilation via different propagators for the process $e^-(p_1) + e^+(p_3) \rightarrow \tilde{\chi}_i^+(p_2) + \tilde{\chi}_j^-(p_4) + H_\ell^0(p_5)$ were investigated and in the Minimal Supersymmetric Standard Model (MSSM), the cross sections for this interaction were estimated. Five groups of 240 probabilities from Feynman diagrams are taken by different propagators. Group (I) when h^0 and Z^0 bosons are propagators, Group (II) when Z^0 and h^0 bosons are propagators, Group (III) when h^0 and h^0 (Lightest Higgs boson) bosons are propagators, Group (IV) Z^0 and Z^0 bosons are propagators and Group (V) $\tilde{\chi}^0$ and Z^0 boson are propagators where $i = j = 1, 2$ and $\ell = 1, 2, 3$.

The process's production cross-sections as a function of mass center energy were calculated, and the best cross-section was based on all considerations of the (MSSM) was determined, the process's mechanisms can be identified as:

$$e^-(P_1) + e^+(P_3) \rightarrow Z^0(P_1 + P_3) \rightarrow Z^0(P_2 + P_4) \rightarrow \tilde{\chi}_i^+(p_2) + \tilde{\chi}_j^-(p_4) \text{ in group I}$$

$$e^-(P_1) + e^+(P_3) \rightarrow Z^0(P_1 + P_3) \rightarrow h^0(P_2 + P_4) \rightarrow \tilde{\chi}_i^+(p_2) + \tilde{\chi}_j^-(p_4) \text{ in group II.}$$

$$e^-(P_1) + e^+(P_3) \rightarrow h^0(P_1 + P_3) \rightarrow h^0(P_2 + P_4) \rightarrow \tilde{\chi}_i^+(p_2) + \tilde{\chi}_j^-(p_4) \text{ in group III}$$

$$e^-(P_1) + e^+(P_3) \rightarrow \tilde{\chi}^0(P_1 + P_3) \rightarrow Z^0(P_2 + P_4) \rightarrow \tilde{\chi}_i^+(p_2) + \tilde{\chi}_j^-(p_4) \text{ in group V}$$

$$e^-(P_1) + e^+(P_3) \rightarrow h^0(P_1 + P_3) \rightarrow Z^0(P_2 + P_4) \rightarrow \tilde{\chi}_i^+(p_2) + \tilde{\chi}_j^-(p_4) \text{ in group I.}$$

At S interval (1600- 3500) Gev, the best value of σ is (7.3934×10^{-4}) Pb in-group (IV). When masses of Charginos are $m_{\tilde{\chi}_j^-} = 900$ GeV, $m_{\tilde{\chi}_i^+} = 700$ GeV and mass of neutral Higgs boson is $m_{H_\ell^0} = 140$ GeV

1. INTRODUCTION

The Supersymmetry Standard Model (SUSY) [1–7], suggests adding a new symmetry to particle physics' Standard Model (SM), as well as a symmetry between bosons and fermions, and anticipates the presence of potential partners for each Standard Model (SM) particle. This provides resolve for the hierarchy dilemma [7-12] and a nominee for dark matter in the form of the lightest supersymmetric particle (LSP), which will be static in the situation of conserved R-parity [13].

The SM's minimal supersymmetric extension (MSSM) [14, 15], The bino, the winos, and the Higgsino

are the superpartners of the $U(1)_Y$ and $SU(2)_L$ gauge fields, as well as the Higgs field. The mass terms for the bino, wino, and Higgsino states are M_1, M_2 , and, μ respectively. Since they do not carry color charge, they can only be produced through electroweak interactions or the decay of colored superpartners. Because electroweak processes have smaller cross sections, the masses of these objects are observationally less limited than the masses of colored SUSY particles. According to the mass spectrum. Through mixing of the superpartners, chargino ($\tilde{\chi}_{1,2}^\pm$) and neutralino ($\tilde{\chi}_{1,2,3,4}^0$) mass eigenstates are created. These are known as electroweakinos, and the subscripts imply increasing electroweakino mass. If the

$\tilde{\chi}_{1,2,3,4}^0$ is stable, for example as the lightest supersymmetric particle (LSP) and R-parity conservation is postulated, it is a viable dark-matter candidate [16, 17].

This paper calculates the cross sections (σ) as a function of center of mass energy a search for direct production of neutral Higgs boson and two charged charginos from electron-positron annihilation via different propagators for the process $e^-(p_1) + e^+(p_3) \rightarrow \tilde{\chi}_i^+(p_2) + \tilde{\chi}_j^-(p_4) + H_i^0(p_5)$

1.1 The Cross-section Scattering

In physics, the significance of cross section is an indicator of the probability that a particular process will occur when a particular type of radiant excitation encounters a highly concentrated phenomenon. The Rutherford cross-section, for example, is an indicator of the chance of an alpha particle being diverted by a specific direction throughout an interaction with an atomic nucleus. σ (sigma) cross section and is measured in term of area, specifically barns. In some ways, it can be compared to the size of the object that the excitation must strike throughout order for the process to take place.

We have learned a lot about nuclear and atomic physics through scattering experiments, such as the discovery of subatomic particles (such as quarks). Scattering phenomena, such as neutron, electron, and x-ray scattering, are used to investigate solid state systems in low energy physics. As a main overview, it is therefore essential in any advanced quantum mechanic's course.

If the radiation is thought to be made up of quanta, the quantity of incident particles hitting the target's surface per unit time per unit area is the flux, and the cross-section measures the scattering rate per unit incident radiation flux. Calculating scattering cross-sections for long-wavelength electromagnetic radiation means dividing the power of the scattered wave by the intensity of the incident wave. A cross-section represents an area in dimensions, with its unit is barn, which has an area of 10^{-28} m^2 . Instead of a true geometric cross-sectional area, a scattering cross-section can be interpreted as an effective area proportional to the probability of interaction between the radiation and the target.

A differential cross section is the differential limit of a function of some final-state parameter, such as particle angle or energy. A total cross section or integrated total

cross section is a cross section that has been integrated over all scattering angles. In a real scattering experiment, the different rates of scattering to different angles provide information about the scatterer. Detectors are positioned at various angles (θ, ϕ). The standard form for an infinitely small solid angle is $d\Omega = \sin\theta d\theta d\phi$. The total solid angle (all probable scatterings) is $\int d\Omega = 4\pi$ the area of a unit radius sphere.

The differential cross section, $d\sigma/d\Omega$, is part of the total number of scattered particles which emerge in the solid angle $d\Omega$, so the rate of particle scattering to this detector is $n d\sigma/d\Omega$, with n defined above as the beam intensity. By integrating over all solid angles, we can obtain the total cross section from the differential.

$$\sigma = \int \frac{d\sigma}{d\Omega} d\Omega = \int_0^{2\pi} d\phi \int_0^\pi d\theta \sin\theta \frac{d\sigma}{d\Omega}$$

The cross section is sensitive to the energy of the incoming particles.

1.2 Properties of Chargino:

Chargino are composed of Winos (W^+, W^-) and Higgsinos (H^+, H^-) [17, 18]. In nature, neutralino dark matter is experimentally investigated indirect through the use of γ ray and neutrino telescopes or directly through the utilizing laboratory experiment like those of Cryogenic dark matter search (CDMS) [19, 20]. Heavier neutralinos usually disintegrate to lighter neutralinos via a neutral Z boson or a via charged W boson to a light chargino. [21]. It is created in pairs through s-channel γ/Z exchange [22, 23]. The lightest neutralino $\tilde{\chi}_1^0$ is heavier than the lightest chargino $\tilde{\chi}_1^\pm$.

The mean lifetime ($\tau_{\tilde{\chi}_1^\pm}$) of $\tilde{\chi}_1^\pm$ is expressed in the form of $\Delta m_{\tilde{\chi}_1}$, which is customarily in the range of a nanosecond. Charginos have a lifetime ranging from 0.1 to 10 ns [24]. The charginos disintegrate to the lightest neutralino $\tilde{\chi}_1^0$, that is believed to be stable, and a two fermions (f) consisting of quarks and antiquarks or leptons and neutrinos [25]. The lightest chargino with a mass larger than 103.5 GeV [26]. There are three variables or soft terms in the chargino mass matrix (M_2, μ and $\tan\beta$) and the neutralino mass matrix has four soft terms (M_1, M_2, μ and $\tan\beta$).

1.3 Higgs boson:

The Standard Model (SM) of elementary particles describes strong and electroweak interactions between

quarks and leptons by exchanging force carriers, such as photons for electromagnetic interactions, W and Z bosons for weak interactions, and gluons for strong interactions. Quarks and leptons serve as the fundamental components of matter in the SM. The electroweak hypothesis unifies the electromagnetic and weak interactions. The SM's predictions have been amply verified because they are remarkably compatible with the majority of accurate measurements up to the energies now available, but it is still unclear how the W and Z gauge bosons pick up mass while the photon stays massless. It was postulated almost 50 years ago that the introduction of a scalar field may lead to spontaneous symmetry breaking in gauge theories. The W and Z masses are produced as a result of applying this method to the electroweak theory through a complex scalar doublet field, and the SM Higgs boson's existence is predicted (H). Through the Yukawa interaction, the scalar field also provides mass to the fundamental fermions [27, 28].

1.3.1 Properties of Higgs boson

The Higgs boson has no spin, has zero electric and color charge and it is also its own antiparticle.

1.4 Two-Higgs-doublet model

Following the breakthrough of the Standard Model (SM) Brout-Englert-Higgs boson at the Large Hadron Collider (LHC), the concern of whether there are more particles within experimental reach remains open.

One straightforward possibility is that a second Higgs doublet has the same quantum numbers as the SM Higgs [29]. The Two-Higgs-Doublet Model (2HDM) is the most basic evolution of the Standard Model (SM), containing one extra scalar doublet with more physical neutral and charged Higgs fields.

There are five physical scalar states with the second Higgs doublet, including the CP even neutral Higgs bosons h and H (where H is heavier than h), the CP odd pseudoscalar A, and two charged Higgs bosons H^\pm . The Higgs boson detected is measured to be CP even. Six physical parameters, including four Higgs masses

m_h, m_H, m_A , and m_{H^\pm} the ratio of the two vacuum expectation values ($\tan\beta$), and the mixing angle (α) that diagonalizes the mass matrix of the neutral CP even Higgses, can be used to characterise such a model. The mass of the Higgs particle and its vacuum expectation value are the only two parameters used by the SM.

$$m_{H^\pm}^2 = \lambda_4(v_1^2 + v_2^2)$$

$$m_A = \lambda_6(v_1^2 + v_2^2)$$

$$m_{H,h}^2 = \frac{1}{2}[a + C \pm D]$$

Were

$$a = 4v_1^2(\lambda_2 + \lambda_3) + v_2^2\lambda_5 \quad ; \quad B = (4\lambda_3 + \lambda_5)v_1v_2 \quad ; \\ C = 4v_2^2(\lambda_2 + \lambda_3) + v_1^2\lambda_5 \quad ; \quad D = \sqrt{(A - C)^2 + 4B^2}$$

λ : wavelength ; v : velocity

The Higgs potential that is composed of quadratic terms and quadratic interaction terms, governs the Higgs characteristics of the MSSM. Supersymmetric gauge couplings directly impact the strength of the interaction terms. The Higgs spectrum, an angle α (which represents the degree of mixing of the original $Y = \pm 1$ Higgs doublet states in the physical CP-even scalars), and the Higgs boson couplings are all determined by $\tan\beta$ and one Higgs mass (m_A).

2. Rules of Calculation Cross sections in (Pb):

Initial states have momenta p_1, p_3 and their masses m_1, m_3 , while three-body final states have momenta p_2, p_4, p_5 and their masses m_2, m_4, m_5 .

$$p_1 + p_3 = p_2 + p_4 + p_5 \quad (1)$$

$$s = \sigma + p_5 \quad (2)$$

The cross section (σ) for the process $e^-(p_1) + e^+(p_3) \rightarrow \tilde{\chi}_i^+(p_2) + \tilde{\chi}_j^-(p_4) + H_\nu^0(p_5)$ can be expressed in writing as

$$\sigma = \int \pi^2 |M|^2 \frac{dx dy d\sigma^2}{\Lambda(S, m_1, m_3)\Lambda(S, \sigma, m_5)} \quad (3)$$

Where M is the matrix element, by using Feynman rules this allows us to write the M-matrix as well as the trace thermos needed to compute the square matrix ($|M|^2$), with the integration carried out by a straightforward approximation produced by an enhanced Weizsacker-Williamson approach [30, 31]. Where:

$$\Lambda(x, y, z) = [x^4 + y^4 + z^4 - 2x^2y^2 - 2x^2z^2 - 2y^2z^2]^{1/2} \quad (4)$$

Then, the integration limit and integration simplification which done by using the Mathematica application are.

$$x_\pm = \frac{1}{4S^2} [(S^2 + m_1^2 - m_3^2)(S^2 - \sigma^2 + m_5^2) \pm \Lambda(S, m_1, m_3)\Lambda(S, \sigma, m_5)] \quad (5)$$

$$y_{\pm} = \frac{1}{4\sigma^2} [(\sigma^2 + m_2^2 - m_4^2)(S^2 - \sigma^2 + m_5^2) \pm \Lambda(\sigma, m_2, m_4)\Lambda(S, \sigma, m_5)] \quad (6)$$

$$(m_2 + m_4)^2 \leq \sigma^2 \leq (S^2 - m_5^2)^2 \quad (7)$$

After calculating the cross sections, the results subsequently charted and reported in tables. We employ the vector-boson masses given by [32] in every one of the computations.

2.1 Constants of the reaction.

$$M_W = 80 \text{ GeV}$$

$$M_Z = 90 \text{ GeV}$$

2.2 New variables of the reaction.

$$M_{H_\ell^0}, \ell = 1, 2, 3 \text{ where } (\ell_1 = M_{h^0}), (\ell_2 = M_{A^0}), (\ell_3 = M_{H^0})$$

$$M_{h^0} = 125 \text{ GeV (mass of } h^0 \text{ propagator)}$$

$$M_{A^0} = 135 \text{ GeV (mass of } A^0 \text{ propagator)}$$

$$M_{H^0} = 140 \text{ GeV (mass of } H^0 \text{ propagator)}$$

$$m_{\tilde{\chi}_j^-} = (800, 900) \text{ GeV}, m_{\tilde{\chi}_i^+} = (600, 700) \text{ GeV } (i, j=1, 2)$$

3. Classified the reaction $e^-(p_1) + e^+(p_3) \rightarrow \tilde{\chi}_i^+(p_2) + \tilde{\chi}_j^-(p_4) + H_\ell^0(p_5)$ according to propagators.

There are five groups from Feynman diagrams classified according to the propagators within (MSSM) models

3.1 Group (I) via h^0 and Z^0 propagators

3.1.1 Feynman Diagram for Group (I)

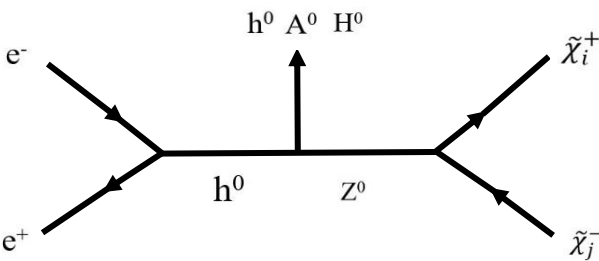


Fig. (1): Feynman diagrams for the process $e^-(p_1) + e^+(p_3) \rightarrow \tilde{\chi}_i^+(p_2) + \tilde{\chi}_j^-(p_4) + H_\ell^0(p_5)$ via h^0 and Z^0 propagators,

3.1.2 Matrix element and Probability of reaction for Group (I)

There should be 48 possibilities from (1– 48) and the

Matrix element is:

$$M_{(1-48)} = (-i(F_L + \gamma_5 F_L)) U_{e^-}(P_1) \bar{V}_{e^+}(P_3) (iG_m(p-q)^\mu) (\sigma^2 - m_Z^2)^{-1} (S^2 - m_h^2)^{-1} (e^{\frac{\cos^2 \theta_w - \sin^2 \theta_w}{2 \sin \theta_w \cos \theta_w}} (P_2 - P_1)) V_{\tilde{\chi}_i^+}(P_2) \bar{U}_{\tilde{\chi}_j^-}(P_4) [33]$$

Where:

g : The gauge coupling constants of $SU(2)_L$

$$g = \frac{e}{\sin \theta_w} = 0.637132$$

m_e : the mass of electron

M_Z : the mass of Z boson

$$M_W = 80 \text{ GeV}$$

$$M_Z = 90 \text{ GeV}$$

$M_{h^0} = 125 \text{ GeV}$ (mass of h^0 propagator, The lightest neutral Higgs boson)

$M_{A^0} = 135 \text{ GeV}$ (mass of A^0 propagator)

$M_{H^0} = 140 \text{ GeV}$ (mass of H^0 propagator, The heaviest neutral Higgs boson)

As, $m_{H_\ell^0}, \ell = 1, 2, 3$ as $\ell = (1=h^0), (2=A^0), (3=H^0)$

$$m_{\tilde{\chi}_j^-} = (800, 900) \text{ GeV}, m_{\tilde{\chi}_i^+} = (600, 700) \text{ GeV } (i, j=1, 2)$$

$$F_L = -g \left(\frac{m_e \cos \alpha}{2 M_W \cos \beta} \right), F_L' = g \left(\frac{m_e \cos \alpha}{2 M_W \cos \beta} \right) [33]$$

$$G_m = i g \left(\frac{\sin(\beta - \alpha)}{2 \cos \theta_w} \right)$$

3.1.3 Cross Section Calculations in (Pb) for Group (I):

In this section we compute the cross sections as a function of center of mass energy for the Feynman diagram in fig. (1) using Feynman rules, equation (3), and the Mathematica software (1). the results shown in figs.2 (a-c) by varying the mass of charginos ($m_{\tilde{\chi}_i^+}, m_{\tilde{\chi}_j^-}$) at different masses of neutral Higgs boson ($M_{h^0}, M_{A^0}, M_{H^0}$)

for the process $e^-(p_1) + e^+(p_3) \rightarrow \tilde{\chi}_i^+(p_2) + \tilde{\chi}_j^-(p_4) + H_\ell^0(p_5)$

$$m_{(\tilde{\chi}_i^+, \tilde{\chi}_j^-)} \rightarrow m_{(600, 800)} \rightarrow m_{11} \text{ (Blue)}$$

$$m_{(\tilde{\chi}_i^+, \tilde{\chi}_j^-)} \rightarrow m_{(600, 900)} \rightarrow m_{12} \text{ (Red)}$$

$$m_{(\tilde{\chi}_i^+, \tilde{\chi}_j^-)} \rightarrow m_{(700, 800)} \rightarrow m_{21} \text{ (Green)}$$

$$m_{(\tilde{\chi}_i^+, \tilde{\chi}_j^-)} \rightarrow m_{(700, 900)} \rightarrow m_{22} \text{ (Pink)}$$

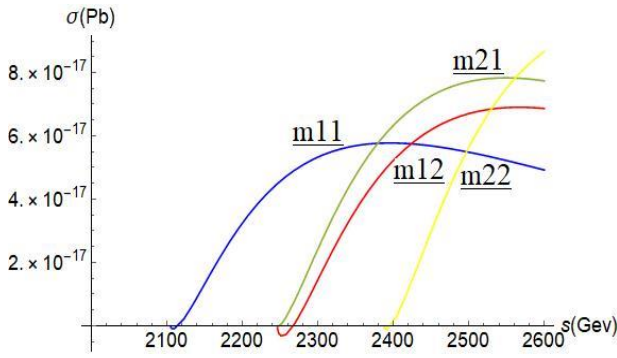


Fig. (2.a) $m_{h^0} = 125 \text{ GeV}$

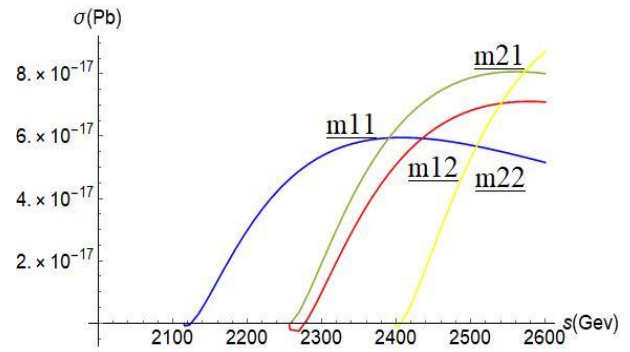


Fig. (2.b) $m_{A^0} = 135 \text{ GeV}$

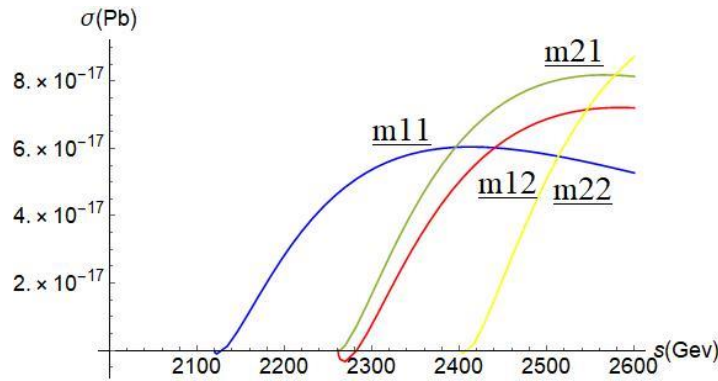


Fig. (2.c) $m_{H^0} = 140 \text{ GeV}$

Fig. (2):The cross sections for the process $e^-(p_1) + e^+(p_3) \rightarrow \tilde{\chi}_i^+(p_2) + \tilde{\chi}_j^-(p_4) + H_\ell^0(p_5)$ as a function of center of mass energy via h^0 and Z^0 bosons propagators by interchanging the mass of Charginos ($m_{\tilde{\chi}_i^+}, m_{\tilde{\chi}_j^-}$) at different mass of neutral Higgs boson ($M_{h^0}, M_{A^0}, M_{H^0}$)

3.1.4 Comparing Results and Discussion for Group (I):

Table (1): Illustrates the comparison between the cross sections for the process $e^-(P_1) + e^+(P_3) \rightarrow h^0(P_1 + P_3) \rightarrow Z^0(P_2 + P_4) \rightarrow \tilde{\chi}_i^+(p_2) + \tilde{\chi}_j^-(p_4)$ via h^0 and Z^0 propagators by interchanging the masses of Charginos ($m_{\tilde{\chi}_i^+}, m_{\tilde{\chi}_j^-}$) at different mass of resultant neutral Higgs boson ($M_{h^0}, M_{A^0}, M_{H^0}$)

$e^-(P_1) + e^+(P_3) \rightarrow h^0(P_1 + P_3) \rightarrow Z^0(P_2 + P_4) \rightarrow \tilde{\chi}_i^+(p_2) + \tilde{\chi}_j^-(p_4)$						
$m_{\tilde{\chi}_i^+}, m_{\tilde{\chi}_j^-}$ $i, j = 1, 2$	Resultant $m_{h^0} = 125$		Resultant $m_{A^0} = 135$		Resultant $m_{H^0} = 140$	
	Fig. (2.a)		Fig. (2.b)		Fig. (2.c)	
	S(Gev)	$\sigma(\text{Pb})$	S(Gev)	$\sigma(\text{Pb})$	S(Gev)	$\sigma(\text{Pb})$
$m_{(\tilde{\chi}_1^+, \tilde{\chi}_2^-)}$ $\rightarrow m_{(600, 800)}$ $\rightarrow m_{11}$	2361.4	5.7271×10^{-17}	2375.2	5.877×10^{-17}	2372.7	5.9544×10^{-17}
$m_{(\tilde{\chi}_1^+, \tilde{\chi}_1^-)}$ $\rightarrow m_{(600, 900)}$ $\rightarrow m_{12}$	2517.1	6.7647×10^{-17}	2525.9	6.9440×10^{-17}	2529.6	7.0650×10^{-17}
$m_{(\tilde{\chi}_1^+, \tilde{\chi}_2^-)}$ $\rightarrow m_{(700, 800)}$ $\rightarrow m_{21}$	2513.3	7.7699×10^{-17}	2520.8	7.9642×10^{-17}	2532.1	8.1103×10^{-17}
$m_{(\tilde{\chi}_1^+, \tilde{\chi}_1^-)}$ $\rightarrow m_{(700, 900)}$ $\rightarrow m_{22}$	2597.4	8.5805×10^{-17}	2599.9	8.6577×10^{-17}	2597.4	8.6003×10^{-17}

By investigation and by the Feynman rules, we computed the cross sections (σ) as a function of center of mass energy (S) for the process $e^-(p_1) + e^+(p_3) \rightarrow \tilde{\chi}_i^+(p_2) + \tilde{\chi}_j^-(p_4) + H_\ell^0(p_5)$ via h^0 and Z^0 propagators. Figs.2 (a-c) show that, as S increase from 1600 to 4000, a maximum value for the cross-sections diverge at various values of Chargino mass ($m_{\tilde{\chi}_i^+}, m_{\tilde{\chi}_j^-}$) and different value of neutral Higgs boson mass ($M_{H^0}, M_{A^0}, M_{H^0}$). From table (1) the best value of σ is (8.6577×10^{-17}) Pb when masses of Charginos are $m_{\tilde{\chi}_j^-} = 900$ GeV, $m_{\tilde{\chi}_i^+} = 700$ GeV and $m_{H_\ell^0} = 135$ GeV

3.2 Group (II) via Z^0 and h^0 are the propagators

3.2.1 Feynman Diagram for Group (II)

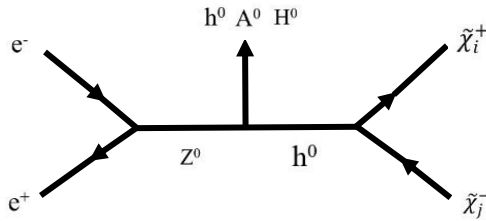


Fig. (3): Feynman diagram for the process $e^-(p_1) + e^+(p_3) \rightarrow \tilde{\chi}_i^+(p_2) + \tilde{\chi}_j^-(p_4) + H_\ell^0(p_5)$ via Z^0 and h^0

3.2.2 Matrix element and probability of reaction for Group (II)

There should be 48 possibilities from (49 – 96) and the Matrix element is:

$$M_{(49-96)} = U_{e^-}(P_1) \bar{V}_{e^+}(P_3) (iG_m(p-q)^\mu) (\sigma^2 - m_h^2)^{-1} (S^2 - m_z^2)^{-1} \left(\frac{-g}{2 \cos \theta_w} \gamma_\alpha \left(\frac{1}{2} - 2Q_i \sin^2 \theta_w - \frac{1}{2} \gamma_5 \right) \right) V_{\tilde{\chi}_i^+}(P_2) \bar{U}_{\tilde{\chi}_j^-}(P_4) (-iY^{\phi_0 \chi_j^+ \chi_i^-}) [33,35]$$

Where:

$$G_m = ig \left(\frac{\sin(\beta-\alpha)}{2 \cos \theta_w} \right)$$

g : The gauge coupling constants of $SU(2)_L$

$$g = \frac{e}{\sin \theta_w} = 0.637132 [34,35]$$

$$Y^{\phi_0 \chi_j^+ \chi_i^-} = \frac{g}{\sqrt{2}} (K_{u\phi}^* U_{i1}^* V_{j2}^* + K_{d\phi}^* U_{i2}^* V_{j1}^*)$$

$$K_{u\phi}^* = (\cos \alpha, \sin \alpha, i \cos \beta, i \sin \beta), K_{d\phi}^* = (-\sin \alpha, \cos \alpha, i \sin \beta, -i \cos \beta)$$

U and V are unitary matrices

$$As, \beta = 56.3, \alpha = -34.48$$

Q_i is a unitary matrix

3.2.3 Cross Section Calculations in (Pb) for Group (II):

The cross sections as a function of center of mass energy for the Feynman diagrams of fig. (3) were calculated and the results are given in fig.4 (a-c) by interchanging the mass of Charginos ($m_{\tilde{\chi}_i^+}, m_{\tilde{\chi}_j^-}$) and the mass of neutral Higgs boson ($M_{H^0}, M_{A^0}, M_{H^0}$)

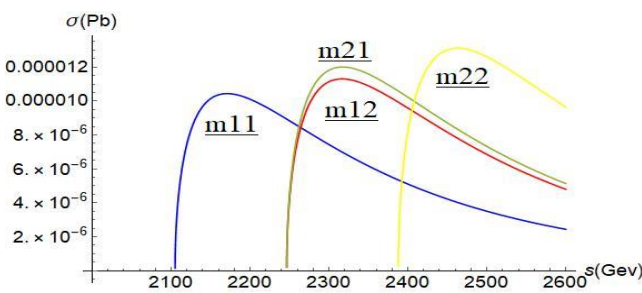


Fig. (4.a) $m_{H^0} = 125$ GeV

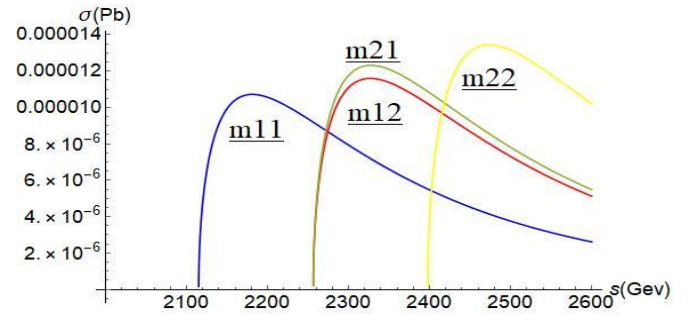


Fig. (4.b) $m_{A^0} = 135$ GeV

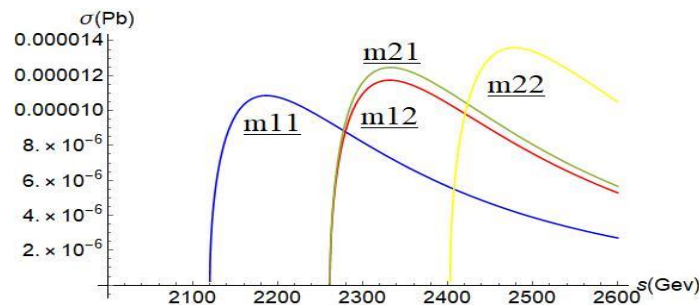


Fig. (4.c) $m_{H^0} = 140$ GeV

Fig.4 (a-c): The cross sections for the process $e^-(p_1) + e^+(p_3) \rightarrow \tilde{\chi}_i^+(p_2) + \tilde{\chi}_j^-(p_4) + H_\ell^0(p_5)$ as a function of center of mass energy via Z^0 and h^0 propagators by interchanging the mass of charginos ($m_{\tilde{\chi}_i^+}, m_{\tilde{\chi}_j^-}$) at different mass of neutral Higgs boson ($M_{H^0}, M_{A^0}, M_{H^0}$)

3.2.4 Comparing Results and Discussion for Group (II):

Table (2): Illustrates the comparison between the cross sections for the process $e^-(P_1) + e^+(P_3) \rightarrow Z^0(P_1 + P_3) \rightarrow h^0(P_2 + P_4) \rightarrow \tilde{\chi}_i^+(p_2) + \tilde{\chi}_j^-(p_4)$ via Z^0 and h^0 propagators by interchanging the masses of Charginos ($m_{\tilde{\chi}_i^+}, m_{\tilde{\chi}_j^-}$) at different mass of resultant neutral Higgs boson ($M_{h^0}, M_{A^0}, M_{H^0}$)

$e^-(P_1) + e^+(P_3) \rightarrow Z^0(P_1 + P_3) \rightarrow h^0(P_2 + P_4) \rightarrow \tilde{\chi}_i^+(p_2) + \tilde{\chi}_j^-(p_4)$						
$m_{\tilde{\chi}_i^+}, m_{\tilde{\chi}_j^-}$ $i, j = 1, 2$	Resultant $m_{h^0} = 125$		Resultant $m_{A^0} = 135$		Resultant $m_{H^0} = 140$	
	Fig. (4.a)		Fig. (4.b)		Fig. (4.c)	
	S(Gev)	σ (Pb)	S(Gev)	σ (Pb)	S(Gev)	σ (Pb)
$m_{(\tilde{\chi}_1^+, \tilde{\chi}_2^-)}$ $\rightarrow m_{(600, 800)}$ $\rightarrow m_{11}$	2167.8	1.0348×10^{-5}	2180.3	1.0651×10^{-5}	2184.1	1.0827×10^{-5}
$m_{(\tilde{\chi}_1^+, \tilde{\chi}_1^-)}$ $\rightarrow m_{(600, 900)}$ $\rightarrow m_{12}$	2315.6	1.1246×10^{-5}	2325.6	1.1571×10^{-5}	2331.9	1.1709×10^{-5}
$m_{(\tilde{\chi}_1^+, \tilde{\chi}_1^-)}$ $\rightarrow m_{(700, 800)}$ $\rightarrow m_{21}$	2315.6	1.1954×10^{-5}	2325.6	1.2249×10^{-5}	2331.9	1.2395×10^{-5}
$m_{(\tilde{\chi}_1^+, \tilde{\chi}_1^-)}$ $\rightarrow m_{(700, 900)}$ $\rightarrow m_{22}$	2463.4	1.3089×10^{-5}	2470.9	1.3363×10^{-5}	2477.2	1.3572×10^{-5}

By investigation and by the Feynman rules, we computed the cross sections (σ) as a function of center of mass energy (S) for the process $e^-(p_1) + e^+(p_3) \rightarrow \tilde{\chi}_i^+(p_2) + \tilde{\chi}_j^-(p_4) + H_\ell^0(p_5)$ via Z^0 and h^0 propagators. Figs.4 (a-c) show that, as S increase from 1600 to 4000, a maximum value for the cross-sections is diverged at varies values of Chargino mass ($m_{\tilde{\chi}_i^+}, m_{\tilde{\chi}_j^-}$) and different value of neutral Higgs boson mass ($M_{h^0}, M_{A^0}, M_{H^0}$). From table (2) the ultimate value of σ is (1.3572×10^{-5}) Pb when masses of Charginos are $m_{\tilde{\chi}_j^-} = 900$ GeV, $m_{\tilde{\chi}_i^+} = 700$ GeV and $m_{H_\ell^0} = 140$ GeV

3.3 Group (III) via h^0 and h^0 are the propagators

3.3.1 Feynman Diagram for Group (III)

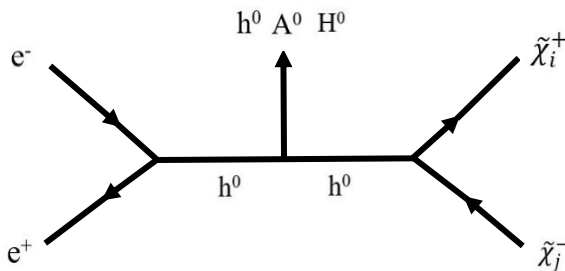


Fig. (5): Feynman diagram for the process $e^-(p_1) + e^+(p_3) \rightarrow \tilde{\chi}_i^+(p_2) + \tilde{\chi}_j^-(p_4) + H_\ell^0(p_5)$ via h^0 and h^0

3.3.2 Matrix element and Probability of reaction for Group (III)

There should be 48 possibilities from (97 – 144) and the Matrix element is:

$$M_{(97-144)} = (-i(F_L + F_L' \gamma_5) U_{e^-}(P_1) \bar{V}_{e^+}(P_3) \left(\frac{-3g m_h^2}{2m_z \cos \theta_w} \right) (\sigma^2 - m_h^2)^{-1} (S^2 - m_h^2)^{-1} \left(\frac{-g m_h^2}{2m_z \cos \theta_w} g^{\alpha\beta} \right) V_{\tilde{\chi}_i^+}(P_2) \bar{U}_{\tilde{\chi}_j^-}(P_4)$$

Where:

$$F_L = -g \left(\frac{m_e \cos \alpha}{2M_W \cos \beta} \right), F_L' = g \left(\frac{m_e \cos \alpha}{2M_W \cos \beta} \right)$$

$g^{\alpha\beta}$ is a (symmetric 4 x 4) metric tensor

3.3.3 Calculation Cross Sections in (Pb) for Group (III):

The Cross sections as a function of center of mass energy for the Feynman diagrams of fig. (5) have been calculated and the results are shown in fig.6 (a-c) by interchanging the mass of ($m_{\tilde{\chi}_i^+}, m_{\tilde{\chi}_j^-}$) and the mass of neutral Higgs boson ($M_{h^0}, M_{A^0}, M_{H^0}$)

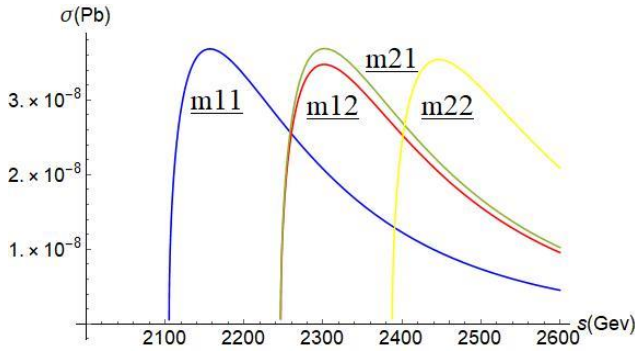


Fig. (6.a) $m_{h^0} = 125 \text{ GeV}$

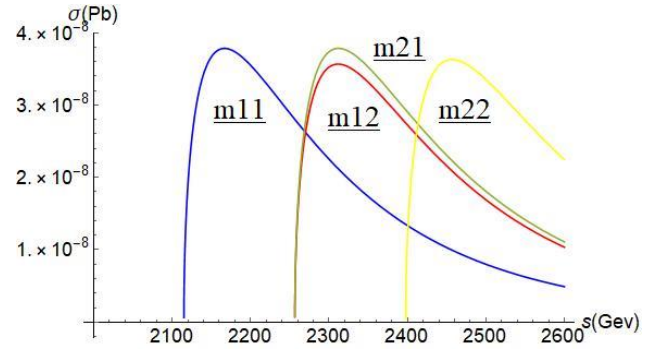


Fig. (6.b) $m_{A^0} = 135 \text{ GeV}$

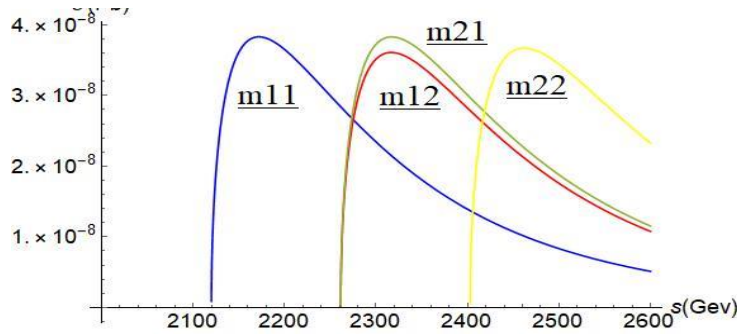


Fig. (6.c) $m_{H^0} = 140 \text{ GeV}$

Fig.6 (a-c): The cross sections for the process $e^-(p_1) + e^+(p_3) \rightarrow \tilde{\chi}_i^+(p_2) + \tilde{\chi}_j^-(p_4) + H_\ell^0(p_5)$ as a function of center of mass energy via h^0 and h^0 propagators by interchanging the mass of ($m_{\tilde{\chi}_i^+}, m_{\tilde{\chi}_j^-}$) and the mass of neutral Higgs boson ($M_{h^0}, M_{A^0}, M_{H^0}$).

3.3.4 Comparing Results and Discussion for Group (III):

Table(3): Illustrates the comparison between the cross sections for the process $e^-(P_1) + e^+(P_3) \rightarrow h^0(P_1 + P_3) \rightarrow h^0(P_2 + P_4) \rightarrow \tilde{\chi}_i^+(p_2) + \tilde{\chi}_j^-(p_4)$ via h^0 and h^0 propagators by interchanging the masses of Charginos ($m_{\tilde{\chi}_i^+}, m_{\tilde{\chi}_j^-}$) at different mass of resultant neutral Higgs boson ($M_{h^0}, M_{A^0}, M_{H^0}$)

$e^-(P_1) + e^+(P_3) \rightarrow h^0(P_1 + P_3) \rightarrow h^0(P_2 + P_4) \rightarrow \tilde{\chi}_i^+(p_2) + \tilde{\chi}_j^-(p_4)$						
$m_{\tilde{\chi}_i^+}, m_{\tilde{\chi}_j^-}$ $i, j = 1, 2$	Resultant $m_{h^0} = 125$		Resultant $m_{A^0} = 135$		Resultant $m_{H^0} = 140$	
	Fig. (6.a)		Fig. (6.b)		Fig. (6.c)	
	S(Gev)	$\sigma(\text{Pb})$	S(Gev)	$\sigma(\text{Pb})$	S(Gev)	$\sigma(\text{Pb})$
$m_{(\tilde{\chi}_1^+, \tilde{\chi}_2^-)}$ $\rightarrow m_{(600, 800)}$ $\rightarrow m_{11}$	2155.3	3.6834×10^{-8}	2165.2	3.7766×10^{-8}	2171.4	3.8104×10^{-8}
$m_{(\tilde{\chi}_1^+, \tilde{\chi}_1^-)}$ $\rightarrow m_{(600, 900)}$ $\rightarrow m_{12}$	2300.6	3.4724×10^{-8}	2311.8	3.5603×10^{-8}	2316.8	3.5914×10^{-8}
$m_{(\tilde{\chi}_1^+, \tilde{\chi}_2^-)}$ $\rightarrow m_{(700, 800)}$ $\rightarrow m_{21}$	2301.9	3.6702×10^{-8}	2313.0	3.7631×10^{-8}	2315.5	3.8241×10^{-8}
$m_{(\tilde{\chi}_1^+, \tilde{\chi}_1^-)}$ $\rightarrow m_{(700, 900)}$ $\rightarrow m_{22}$	2447.2	3.5383×10^{-8}	2457.2	3.6144×10^{-8}	2463.4	3.6461×10^{-8}

By investigation and by the Feynman rules, we computed the cross sections (σ) as a function of center of mass energy (S) for the process $e^-(p_1) + e^+(p_3) \rightarrow \tilde{\chi}_i^+(p_2) + \tilde{\chi}_j^-(p_4) + H_\ell^0(p_5)$ via h^0 and h^0 propagators. Figs.6 (a-c) show that, at S increase from 1600 to 3500, the maximum value for the cross-sections diverge at various values of Chargino mass ($m_{\tilde{\chi}_i^+}, m_{\tilde{\chi}_j^-}$) and different value of neutral Higgs boson mass ($M_{H^0}, M_{A^0}, M_{H^0}$). From table (3) the best value of σ is (3.8241×10^{-8}) Pb when masses of Charginos are $m_{\tilde{\chi}_j^-} = 800$ GeV, $m_{\tilde{\chi}_i^+} = 700$ GeV and $m_{H_\ell^0} = 140$ GeV

3.4 Group (IV) Z^0 and Z^0 are the propagators

3.4.1 Feynman Diagram for Group (IV)

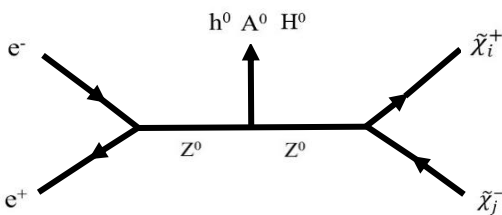


Fig. (7): Feynman diagram for the process $e^-(p_1) + e^+(p_3) \rightarrow \tilde{\chi}_i^+(p_2) + \tilde{\chi}_j^-(p_4) + H_\ell^0(p_5)$ via Z^0 and Z^0

3.4.2 Matrix element and Probability of reaction for Group (IV)

There should be 48 possibilities from (145 – 192) and the Matrix element is:

$$M_{(145-192)} = \left(\frac{-g}{2 \cos \theta_w} \gamma_\alpha \left(\frac{1}{2} - 2Q_i \sin^2 \theta_w - \frac{1}{2} \gamma_5 \right) U_{e^-}(P_1) \bar{V}_{e^+}(P_3) \left(ig \left(\frac{m_Z \cos(\beta - \alpha)}{\cos \theta_w} \right) g^{\mu\nu} \right) (\sigma^2 - m_Z^2)^{-1} (S^2 - m_Z^2)^{-1} \left(e \frac{\cos^2 \theta_w - \sin^2 \theta_w}{2 \sin \theta_w \cos \theta_w} (P_2 - P_1) \right) V_{\tilde{\chi}_i^+}(P_2) \bar{U}_{\tilde{\chi}_j^-}(P_4) \right) [35,36]$$

Where:

Q_i is a unitary matrix, $g^{\mu\nu}$ is a (symmetric 4 x 4) metric tensor
 $A_s, \beta = 56.3, \alpha = -34.48, \theta_w = 28.7, e = 0.302822$

3.4.3 Cross Section Calculations in (Pb) for Group (IV):

The cross sections as a function of center of mass energy for the Feynman diagrams of fig. (7) have been calculated and the results are shown in fig.8 (a-c) by interchanging the mass of charginos ($m_{\tilde{\chi}_i^+}, m_{\tilde{\chi}_j^-}$) and the mass of neutral Higgs boson ($M_{H^0}, M_{A^0}, M_{H^0}$)

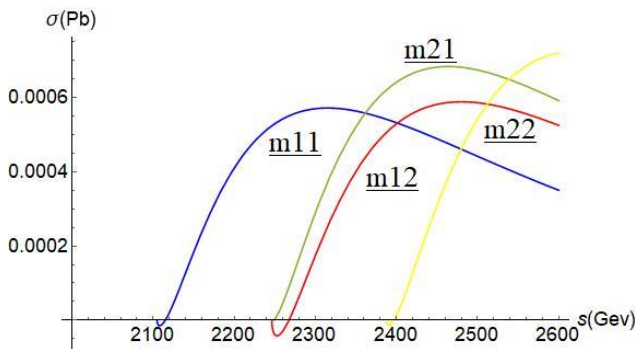


Fig. (8.a) $m_{H^0} = 125$ GeV

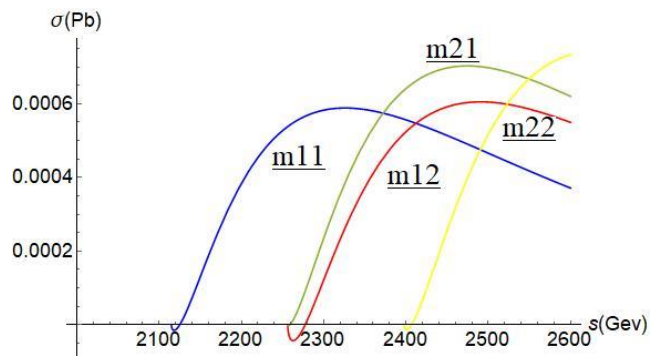


Fig. (8.b) $m_{A^0} = 135$ GeV

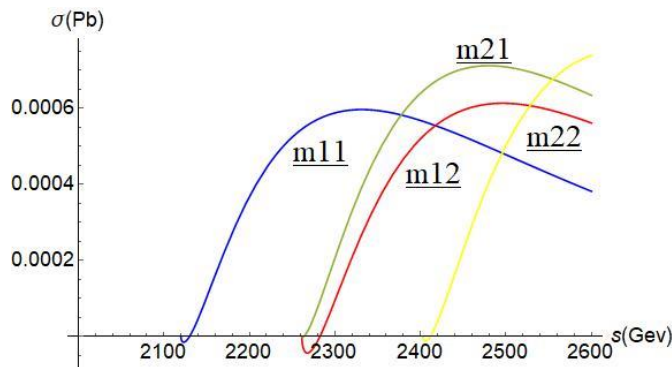


Fig. (8.c) $m_{H^0} = 140$ GeV

Fig.8 (a-c): The cross sections for the process $e^-(p_1) + e^+(p_3) \rightarrow \tilde{\chi}_i^+(p_2) + \tilde{\chi}_j^-(p_4) + H_\ell^0(p_5)$ as a function of center of mass energy via Z^0 and Z^0 propagators by interchanging the mass of ($m_{\tilde{\chi}_i^+}, m_{\tilde{\chi}_j^-}$) and the mass of neutral Higgs boson ($M_{H^0}, M_{A^0}, M_{H^0}$).

3.4.4 Comparing Results and Discussion for Group (IV):

Table(4): Illustrates the comparison between the cross sections for the process $e^-(P_1) + e^+(P_3) \rightarrow Z^0(P_1 + P_3) \rightarrow Z^0(P_2 + P_4) \rightarrow \tilde{\chi}_i^+(p_2) + \tilde{\chi}_j^-(p_4)$ via Z^0 and Z^0 propagators by interchanging the masses of Charginos ($m_{\tilde{\chi}_i^+}, m_{\tilde{\chi}_j^-}$) at different mass of resultant neutral Higgs boson ($M_{h^0}, M_{A^0}, M_{H^0}$)

$e^-(P_1) + e^+(P_3) \rightarrow Z^0(P_1 + P_3) \rightarrow Z^0(P_2 + P_4) \rightarrow \tilde{\chi}_i^+(p_2) + \tilde{\chi}_j^-(p_4)$						
$m_{\tilde{\chi}_i^+}, m_{\tilde{\chi}_j^-}$ $i, j = 1, 2$	Resultant $m_{h^0}=125$		Resultant $m_{A^0}=135$		Resultant $m_{H^0}=140$	
	Fig. (8.a)		Fig. (8.b)		Fig. (8.c)	
	S(Gev)	σ (Pb)	S(Gev)	σ (Pb)	S(Gev)	σ (Pb)
$m_{(\tilde{\chi}_1^+, \tilde{\chi}_1^-)}$ $\rightarrow m_{(600, 800)}$ $\rightarrow m_{11}$	2303.1	5.6681×10^{-4}	2316.6	5.8589×10^{-4}	2323.9	5.9607×10^{-4}
$m_{(\tilde{\chi}_1^+, \tilde{\chi}_2^-)}$ $\rightarrow m_{(600, 900)}$ $\rightarrow m_{12}$	2465.7	5.8557×10^{-4}	2478.0	5.9955×10^{-4}	2480.4	6.0985×10^{-4}
$m_{(\tilde{\chi}_2^+, \tilde{\chi}_1^-)}$ $\rightarrow m_{(700, 800)}$ $\rightarrow m_{21}$	2457.2	6.8206×10^{-4}	2470.6	7.0339×10^{-4}	2475.5	7.1179×10^{-4}
$m_{(\tilde{\chi}_2^+, \tilde{\chi}_2^-)}$ $\rightarrow m_{(700, 900)}$ $\rightarrow m_{22}$	2596.6	7.1690×10^{-4}	2600.2	7.3345×10^{-4}	2600.2	7.3934×10^{-4}

By investigation and by the Feynman rules, we computed the cross sections (σ) as a function of center of mass energy (S) for the process $e^-(p_1) + e^+(p_3) \rightarrow \tilde{\chi}_i^+(p_2) + \tilde{\chi}_j^-(p_4) + H_\ell^0(p_5)$ via Z^0 and Z^0 propagators. Figs.8 (a-c) show that, as S increases from 1600 to 3500, the maximum value for the cross-sections diverge at varies values of Chargino mass ($m_{\tilde{\chi}_i^+}, m_{\tilde{\chi}_j^-}$) and different value of neutral Higgs boson mass ($M_{h^0}, M_{A^0}, M_{H^0}$). From Table (4) the best value of σ is (7.3934×10^{-4}) Pb when masses of Charginos are $m_{\tilde{\chi}_j^-} = 900$ GeV, $m_{\tilde{\chi}_i^+} = 700$ GeV and $m_{H_\ell^0} = 140$ GeV

3.5 Group (V) via $\tilde{\chi}^0$ and Z^0 are the propagators

3.5.1 Feynman Diagram for Group (V)

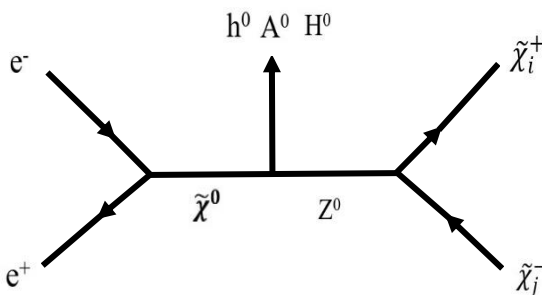


Fig. (9): Feynman diagram for the process $e^-(p_1) + e^+(p_3) \rightarrow \tilde{\chi}_i^+(p_2) + \tilde{\chi}_j^-(p_4) + H_\ell^0(p_5)$ via $\tilde{\chi}^0$ and Z^0

3.5.2 Matrix element and Probability of reaction for Group (V)

There should be 48 possibilities from (193-240) and the Matrix element is:

$$M_{(193-240)} = (-i e \frac{1}{2 \sin \theta_w} \frac{m_f}{m_w} \gamma_5) U_{e^-}(P_1) \bar{V}_{e^+}(P_3) \left(\frac{i e}{2 \sin \theta_w \cos \theta_w} ((1 - \varepsilon) P_2 - (1 + \varepsilon) P_4) \right) (\sigma^2 - m_{\tilde{\chi}_i^+}^2)^{-1} (S^2 - m_{\tilde{\chi}_j^-}^2)^{-1} (e \frac{\cos^2 \theta_w - \sin^2 \theta_w}{2 \sin \theta_w \cos \theta_w} (P_2 - P_1)) V_{\tilde{\chi}_i^+}(P_2) \bar{U}_{\tilde{\chi}_j^-}(P_4) [37,38]$$

Where:

m_f , is mass of electron = 0.000511 GeV/C², $m_w = 80$ GeV/C²

$\varepsilon_{ij} = 1$, because we use different masses of charginos, $e = 0.302822$

3.5.3 Cross Section Calculations in (Pb) for Group (V):

The cross sections as a function of the center of mass energy for the Feynman diagrams of Fig. (9) have been calculated and the results are shown in Fig.10 (a-c) by interchanging the mass of charginos ($m_{\tilde{\chi}_i^+}, m_{\tilde{\chi}_j^-}$) and the mass of neutral Higgs boson ($M_{h^0}, M_{A^0}, M_{H^0}$)

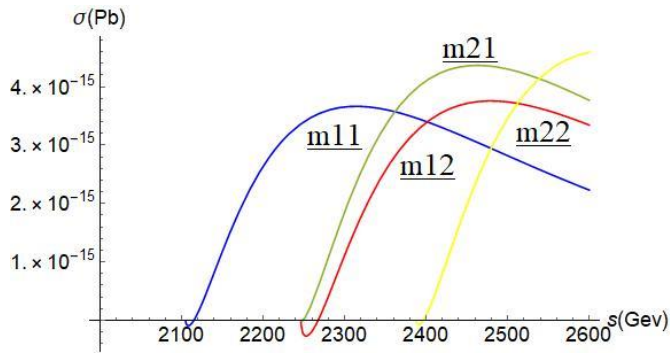
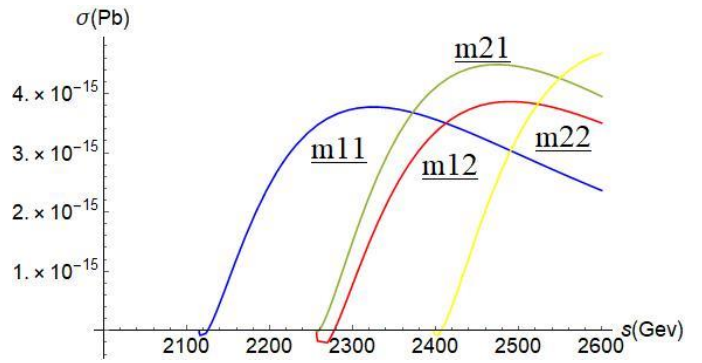
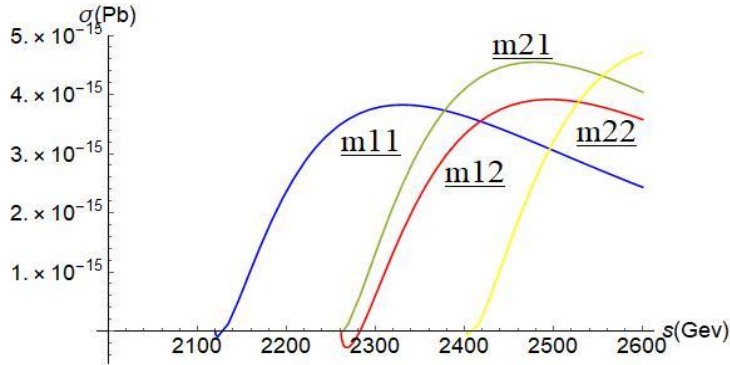
Fig. (10.a) $m_{h^0} = 125$ GeVFig. (10.b) $M_{A^0} = 135$ GeVFig. (10.c) $M_{H^0} = 140$ GeV

Fig.10(a-c): The cross sections for the process $e^-(p_1) + e^+(p_3) \rightarrow \tilde{\chi}_i^+(p_2) + \tilde{\chi}_j^-(p_4) + H^0(p_5)$ as a function of center of mass energy via $\tilde{\chi}^0$ and Z^0 propagators by interchanging the mass of $(m_{\tilde{\chi}_i^+}, m_{\tilde{\chi}_j^-})$ and the mass of neutral Higgs boson $(M_{h^0}, M_{A^0}, M_{H^0})$.

3.5.4 Comparing Results and Discussion for Group (V):

Table(5): Illustrates the comparison between the cross sections for the process $e^-(P_1) + e^+(P_3) \rightarrow \tilde{\chi}^0(P_1 + P_3) \rightarrow Z^0(P_2 + P_4) \rightarrow \tilde{\chi}_i^+(p_2) + \tilde{\chi}_j^-(p_4)$ via $\tilde{\chi}^0$ and Z^0 propagators by interchanging the masses of Charginos $(m_{\tilde{\chi}_i^+}, m_{\tilde{\chi}_j^-})$ at different mass of resultant neutral Higgs boson $(M_{h^0}, M_{A^0}, M_{H^0})$.

$e^-(P_1) + e^+(P_3) \rightarrow \tilde{\chi}^0(P_1 + P_3) \rightarrow Z^0(P_2 + P_4) \rightarrow \tilde{\chi}_i^+(p_2) + \tilde{\chi}_j^-(p_4)$						
$m_{\tilde{\chi}_i^+}, m_{\tilde{\chi}_j^-}$ $i, j = 1, 2$	Resultant $m_{h^0} = 125$		Resultant $M_{A^0} = 135$		Resultant $M_{H^0} = 140$	
	Fig. (10.a)		Fig. (10.b)		Fig. (10.c)	
	S(Gev)	σ (Pb)	S(Gev)	σ (Pb)	S(Gev)	σ (Pb)
$m(\tilde{\chi}_1^+, \tilde{\chi}_1^-)$ $\rightarrow m_{(600, 800)}$ $\rightarrow m_{11}$	2299.9	3.6296×10^{-15}	2312.5	3.7490×10^{-15}	2322.5	3.8017×10^{-15}
$m(\tilde{\chi}_1^+, \tilde{\chi}_2^-)$ $\rightarrow m_{(600, 900)}$ $\rightarrow m_{12}$	2466.9	3.7348×10^{-15}	2475.6	3.8371×10^{-15}	2485.7	3.8918×10^{-15}
$m(\tilde{\chi}_2^+, \tilde{\chi}_1^-)$ $\rightarrow m_{(700, 800)}$ $\rightarrow m_{21}$	2453.1	4.3486×10^{-15}	2470.6	4.4712×10^{-15}	2475.6	4.5401×10^{-15}
$m(\tilde{\chi}_2^+, \tilde{\chi}_2^-)$ $\rightarrow m_{(700, 900)}$ $\rightarrow m_{22}$	2596.1	4.5590×10^{-15}	2598.6	4.6473×10^{-15}	2598.6	4.6842×10^{-15}

By investigation and by the Feynman rules, we computed the cross sections (σ) as a function of center of mass energy (S) for the process $e^-(p_1) + e^+(p_3) \rightarrow \tilde{\chi}_i^+(p_2) + \tilde{\chi}_j^-(p_4) + H_\ell^0(p_5)$ via $\tilde{\chi}^0$ and Z^0 propagators. Figs.10 (a-c) show that, as S increase from 1600 to 3500, a maximum value for the cross-sections is diverge at varies values of Chargino mass ($m_{\tilde{\chi}_i^+}, m_{\tilde{\chi}_j^-}$) and different value of neutral Higgs boson mass ($M_{H^0}, M_{A^0}, M_{H^0}$). From table (5) the best value of σ is (4.6842×10^{-15}) Pb when masses of Charginos are $m_{\tilde{\chi}_j^-} = 900$ GeV, $m_{\tilde{\chi}_i^+} = 700$ GeV and $m_{H_\ell^0} = 140$ GeV

4. RESULTS AND DISCUSSION

Based on the investigation of the production of neutral Higgs boson and two charged charginos from electron – positron annihilation via different propagators for interaction $e^-(p_1) + e^+(p_3) \rightarrow \tilde{\chi}_i^+(p_2) + \tilde{\chi}_j^-(p_4) + H_\ell^0(p_5)$ we can study the cross-sections σ (Pb) as a function of center of mass energy S (GeV). We estimated the cross sections for this interaction in the Minimal Supersymmetric Standard Model (MSSM).

We draw all Feynman diagrams probabilities for the reaction $e^-(p_1) + e^+(p_3) \rightarrow \tilde{\chi}_i^+(p_2) + \tilde{\chi}_j^-(p_4) + H_\ell^0(p_5)$ arranged according to the propagators, we have 180 probabilities of the reaction divided into five groups.

Groupe (I) Production via h^0 and Z^0 propagators,

$$e^-(P_1) + e^+(P_3) \rightarrow h^0(P_1 + P_3) \rightarrow Z^0(P_2 + P_4) \rightarrow$$

$$\tilde{\chi}_i^+(p_2) + \tilde{\chi}_j^-(p_4)$$

Groupe (II) Production via Z^0 and h^0 propagators,

$$e^-(P_1) + e^+(P_3) \rightarrow Z^0(P_1 + P_3) \rightarrow h^0(P_2 + P_4) \rightarrow \tilde{\chi}_i^+(p_2) + \tilde{\chi}_j^-(p_4)$$

Groupe (III) Production via h^0 and h^0 propagators,

$$e^-(P_1) + e^+(P_3) \rightarrow h^0(P_1 + P_3) \rightarrow h^0(P_2 + P_4) \rightarrow \tilde{\chi}_i^+(p_2) + \tilde{\chi}_j^-(p_4)$$

Groupe (IV) Production via Z^0 and Z^0 propagators,

$$e^-(P_1) + e^+(P_3) \rightarrow Z^0(P_1 + P_3) \rightarrow Z^0(P_2 + P_4) \rightarrow \tilde{\chi}_i^+(p_2) + \tilde{\chi}_j^-(p_4)$$

Groupe (V) Production via h^0 and Z^0 propagators,

$$e^-(P_1) + e^+(P_3) \rightarrow \tilde{\chi}^0(P_1 + P_3) \rightarrow Z^0(P_2 + P_4) \rightarrow \tilde{\chi}_i^+(p_2) + \tilde{\chi}_j^-(p_4)$$

We calculated the cross – sections σ (Pb) as a function of the center of mass energy S (GeV) at different values of Chargino mass ($m_{\tilde{\chi}_i^+}, m_{\tilde{\chi}_j^-}$) where, $m_{(\tilde{\chi}_i^+, \tilde{\chi}_j^-)} \rightarrow m_{(600,800)}, m_{(\tilde{\chi}_i^+, \tilde{\chi}_j^-)} \rightarrow m_{(600,900)}, m_{(\tilde{\chi}_i^+, \tilde{\chi}_j^-)} \rightarrow m_{(700,800)}, m_{(\tilde{\chi}_i^+, \tilde{\chi}_j^-)} \rightarrow m_{(700,900)}$, and different values of neutral Higgs boson mass ($M_{H^0} = 125$ GeV, $M_{A^0} = 135$ GeV, $M_{H^0} = 140$ GeV) for five groups.

And draw the cross—sections as a function of incident energy for all probabilities, there are 60 curves.

By comparing the results of the peak values for cross- sections of all curves we found that:

Table (6): The peak values of the cross sections of the interaction $e^-(p_1) + e^+(p_3) \rightarrow \tilde{\chi}_i^+(p_2) + \tilde{\chi}_j^-(p_4) + H_\ell^0(p_5)$ via different propagators, with different masses of Charginos ($m_{\tilde{\chi}_i^+}, m_{\tilde{\chi}_j^-}$) and neutral Higgs boson mass M_{H^0} at different values of incident energies for five groups.

Group NO	$e^-(p_1) + e^+(p_3) \rightarrow \tilde{\chi}_i^+(p_2) + \tilde{\chi}_j^-(p_4) + H_\ell^0(p_5)$	Fig. no.	m_{h^0, A^0, H^0} (GeV)	$m_{\tilde{\chi}_i^+} m_{\tilde{\chi}_j^-}$ (GeV/ C ²)	S (GeV)	σ_{max} (Pb)
1 st	Production via h^0 and Z^0 $e^-(P_1) + e^+(P_3) \rightarrow h^0(P_1 + P_3) \rightarrow Z^0(P_2 + P_4) \rightarrow \tilde{\chi}_i^+(p_2) + \tilde{\chi}_j^-(p_4)$	2.b	$m_{H^0} = 135$ GeV	700,900	2599.9	8.6577×10^{-17}
2 nd	Production via Z^0 and h^0 $e^-(P_1) + e^+(P_3) \rightarrow Z^0(P_1 + P_3) \rightarrow h^0(P_2 + P_4) \rightarrow \tilde{\chi}_i^+(p_2) + \tilde{\chi}_j^-(p_4)$	4.c	$m_{H^0} = 140$ GeV	700,900	2477.2	1.3572×10^{-5}
3 rd	Production via h^0 and h^0 $e^-(P_1) + e^+(P_3) \rightarrow h^0(P_1 + P_3) \rightarrow h^0(P_2 + P_4) \rightarrow \tilde{\chi}_i^+(p_2) + \tilde{\chi}_j^-(p_4)$	6.c	$m_{H^0} = 140$ GeV	700,800	2315.5	3.8241×10^{-8}
4 th	Production via Z^0 and Z^0 $e^-(P_1) + e^+(P_3) \rightarrow Z^0(P_1 + P_3) \rightarrow Z^0(P_2 + P_4) \rightarrow \tilde{\chi}_i^+(p_2) + \tilde{\chi}_j^-(p_4)$	8.c	$m_{H^0} = 140$ GeV	700,900	2600.2	7.3934×10^{-4}
5 th	Production via $\tilde{\chi}^0$ and Z^0 $e^-(P_1) + e^+(P_3) \rightarrow \tilde{\chi}^0(P_1 + P_3) \rightarrow Z^0(P_2 + P_4) \rightarrow \tilde{\chi}_i^+(p_2) + \tilde{\chi}_j^-(p_4)$	10.c	$m_{H^0} = 140$ GeV	700,900	2598.6	4.6842×10^{-15}

The dominant process

Is Group (IV), $e^-(P_1) + e^+(P_3) \rightarrow Z^0(P_1 + P_3) \rightarrow Z^0(P_2 + P_4) \rightarrow \tilde{\chi}_i^+(p_2) + \tilde{\chi}_j^-(p_4)$

in which S interval (1600- 3500) GeV, the best value of σ is (7.3934×10^{-4}) Pb. When masses of Charginos are $m_{\tilde{\chi}_j^-} = 900$ GeV, $m_{\tilde{\chi}_i^+} = 700$ GeV and mass of neutral Higgs boson is $m_{H_\rho^0} = 140$ GeV

The competing process

Is Group (II), $e^-(P_1) + e^+(P_3) \rightarrow Z^0(P_1 + P_3) \rightarrow h^0(P_2 + P_4) \rightarrow \tilde{\chi}_i^+(p_2) + \tilde{\chi}_j^-(p_4)$

in which S interval (1600- 4000) GeV, the best value of σ is (1.3572×10^{-5}) Pb. When masses of Charginos are $m_{\tilde{\chi}_j^-} = 900$ GeV, $m_{\tilde{\chi}_i^+} = 700$ GeV and mass of neutral Higgs boson is $m_{H_\rho^0} = 140$ GeV

And the other processes

Are Group (III), $e^-(P_1) + e^+(P_3) \rightarrow h^0(P_1 + P_3) \rightarrow h^0(P_2 + P_4) \rightarrow \tilde{\chi}_i^+(p_2) + \tilde{\chi}_j^-(p_4)$

in which S interval (1600- 3500) GeV, the best value of σ is (3.8241×10^{-8}) Pb. When masses of Charginos are $m_{\tilde{\chi}_j^-} = 800$ GeV, $m_{\tilde{\chi}_i^+} = 700$ GeV and mass of neutral Higgs boson is $m_{H_\rho^0} = 140$ GeV

Group (V), $e^-(P_1) + e^+(P_3) \rightarrow \tilde{\chi}^0(P_1 + P_3) \rightarrow Z^0(P_2 + P_4) \rightarrow \tilde{\chi}_i^+(p_2) + \tilde{\chi}_j^-(p_4)$

in which S interval (1600- 3500) GeV, the best value of σ is (4.6842×10^{-15}) Pb. When masses of Charginos are $m_{\tilde{\chi}_j^-} = 900$ GeV, $m_{\tilde{\chi}_i^+} = 700$ GeV and mass of neutral Higgs boson is $m_{H_\rho^0} = 140$ GeV

Group (I), $e^-(P_1) + e^+(P_3) \rightarrow h^0(P_1 + P_3) \rightarrow Z^0(P_2 + P_4) \rightarrow \tilde{\chi}_i^+(p_2) + \tilde{\chi}_j^-(p_4)$

in which S interval (1600- 4000) GeV, the best value of σ is (8.6577×10^{-17}) Pb. When masses of Charginos are $m_{\tilde{\chi}_j^-} = 900$ GeV, $m_{\tilde{\chi}_i^+} = 700$ GeV and mass of neutral Higgs boson is $m_{H_\rho^0} = 135$ GeV

5. CONCLUSION

Identifying the scenario with the highest cross-section for the reaction was successfully investigated. $e^-(p_1) + e^+(p_3) \rightarrow \tilde{\chi}_i^+(p_2) + \tilde{\chi}_j^-(p_4) + H_\rho^0(p_5)$. The cross-sections for this interaction in the Minimal Supersymmetric Model (MSSM) were calculated. Our results show that the best cross section increases to (7.3934×10^{-4}) Pb at $(S = 2600.2)$ GeV when masses of Charginos are $m_{\tilde{\chi}_j^-} = 900$ GeV, $m_{\tilde{\chi}_i^+} = 700$ GeV and mass of neutral Higgs boson is $m_{H_\rho^0} = 140$ GeV, via Z^0

and Z^0 boson propagators exchange in Fig. (3.c) for the reaction Production via Z^0 and Z^0

$e^-(P_1) + e^+(P_3) \rightarrow Z^0(P_1 + P_3) \rightarrow Z^0(P_2 + P_4) \rightarrow \tilde{\chi}_i^+(p_2) + \tilde{\chi}_j^-(p_4)$ in group (IV)

REFERENCES

- [1] Y. Golfand and E. Likhtman, Extension of the Algebra of Poincare Group Generators and Violation of P Invariance, JETP Lett. 13 (1971) 323, [Pisma Zh. Eksp. Teor. Fiz. 13 (1971) 452].
https://doi.org/10.1142/9789814542340_0001
- [2] D. Volkov and V. Akulov, Is the neutrino a goldstone particle?, Phys. Lett. B 46 (1973) 109.
[https://doi.org/10.1016/0370-2693\(73\)90490-5](https://doi.org/10.1016/0370-2693(73)90490-5)
- [3] J. Wess and B. Zumino, Supergauge transformations in four dimensions, Nucl. Phys. B 70 (1974) 39.
[https://doi.org/10.1016/0550-3213\(74\)90355-1](https://doi.org/10.1016/0550-3213(74)90355-1)
- [4] J. Wess and B. Zumino, Supergauge invariant extension of quantum electrodynamics, Nucl. Phys. B 78 (1974) 1.
[https://doi.org/10.1016/0550-3213\(74\)90112-6](https://doi.org/10.1016/0550-3213(74)90112-6)
- [5] S. Ferrara and B. Zumino, Supergauge invariant Yang-Mills theories, Nucl. Phys. B 79 (1974) 413.
[https://doi.org/10.1016/0550-3213\(74\)90559-8](https://doi.org/10.1016/0550-3213(74)90559-8)
- [6] A. Salam and J. Strathdee, Super-symmetry and non-Abelian gauges, Phys. Lett. B 51 (1974) 353.
[https://doi.org/10.1016/0370-2693\(74\)90226-3](https://doi.org/10.1016/0370-2693(74)90226-3)
- [7] Ankush Reddy Kanuganti search for electroweak production of charginos and neutralinos in all hadronic final states at the cms experiment, arXiv:2205.15711v1 [hep-ex] 31 May 2022
<https://doi.org/10.48550/arXiv.2205.15711>
- [8] L. Girardello and M. T. Grisaru, Soft Breaking of Supersymmetry, Nucl. Phys. B 194 (1982) 65.
[https://doi.org/10.1016/0550-3213\(82\)90512-0](https://doi.org/10.1016/0550-3213(82)90512-0)
- [9] N. Sakai, Naturalness in supersymmetric GUTS, Z. Phys. C 11 (1981) 153.
<https://doi.org/10.1007/BF01573998>
- [10] S. Dimopoulos, S. Raby and F. Wilczek, Supersymmetry and the scale of unification, Phys. Rev. D 24 (1981) 1681.
<https://doi.org/10.1103/PhysRevD.24.1681>
- [11] L. E. Ibáñez and G. G. Ross, Low-energy predictions in supersymmetric grand unified theories, Phys. Lett. B 105 (1981) 439.
[https://doi.org/10.1016/0370-2693\(81\)91200-4](https://doi.org/10.1016/0370-2693(81)91200-4)
- [12] S. Dimopoulos and H. Georgi, Softly broken supersymmetry and SU(5), Nucl. Phys. B 193 (1981) 150.
[https://doi.org/10.1016/0550-3213\(81\)90522-8](https://doi.org/10.1016/0550-3213(81)90522-8)
- [13] G. R. Farrar and P. Fayet, Phenomenology of the production, decay, and detection of new hadronic states associated with supersymmetry, Phys. Lett. B 76 (1978)

575.
[https://doi.org/10.1016/0370-2693\(78\)90858-4](https://doi.org/10.1016/0370-2693(78)90858-4)
- [14] P. Fayet, Supersymmetry and weak, electromagnetic and strong interactions, Phys. Lett. B 64 (1976) 159.
[https://doi.org/10.1016/0370-2693\(76\)90319-1](https://doi.org/10.1016/0370-2693(76)90319-1)
- [15] P. Fayet, spontaneously broken supersymmetric theories of weak, electromagnetic and strong interactions, Phys. Lett. B 69 (1977) 489.
[https://doi.org/10.1016/0370-2693\(77\)90852-8](https://doi.org/10.1016/0370-2693(77)90852-8)
- [16] H. Goldberg, Constraint on the Photino Mass from Cosmology, Phys. Rev. Lett. 50 (1983) 1419, Erratum: Phys. Rev. Lett. 103 (2009) 099905.
<https://doi.org/10.1103/PhysRevLett.103.099905>
- [17] J. Ellis, J. Hagelin, D. V. Nanopoulos, K. A. Olive and M. Srednicki, Supersymmetric relics from the big bang, Nucl. Phys. B 238 (1984) 453.
[https://doi.org/10.1016/0550-3213\(84\)90461-9](https://doi.org/10.1016/0550-3213(84)90461-9)
- [18] Aldufeery E, Binjonaid M. Dark matter constraints and the neutralino sector of the scNMSSM. Universe. (2021);7(2):31
<https://doi.org/10.3390/universe7020031>
- [19] Martin, Stephen P. A supersymmetry primer. In: Perspectives on supersymmetry. (1998). p. 1-98.
https://doi.org/10.1142/9789812839657_0001
- [20] Bertone, Gianfranco (ed.). Particle dark matter: observations, models and searches. Cambridge University Press, (2010).
<https://doi.org/10.1017/CBO9780511770739>
- [21] Heuer, R.-D., et al. TESLA technical design report part III: Physics at an e^+e^- linear collider. arXiv preprint hep-ph/0106315, (2001).
<https://doi.org/10.48550/arXiv.hep-ph/0106315>
- [22] de Vera MT, Berggren M, List J. Chargino production at the ILC. arXiv preprint arXiv:2002.01239. (2020)
<https://doi.org/10.48550/arXiv.2002.01239>
- [23] AAD, Georges, et al. Search for charginos nearly mass degenerate with the lightest neutralino based on a disappearing-track signature in $p\bar{p}$ collisions at $\sqrt{s}=8$ TeV with the ATLAS detector. Physical Review D, (2013), 88.11: 112006.
<https://doi.org/10.1103/PhysRevD.88.112006>
- [24] Choi, S. Y., et al. Chargino pair production in e^-e^+ collisions. The European Physical Journal C-Particles and Fields, (1999), 7.1: 123-134.
<https://doi.org/10.1007/s100529800957>
- [25] H.Baer, V.Barger and H.Serçe (2019) [hep-ph/1907.06693v1].
<https://doi.org/10.1103/PhysRevD.94.115019>
- [26] LI, Tianjun. Determining M_1, M_2, μ and $\tan\beta$ in MSSM from Chargino and Neutralino Masses. (1998).
<https://doi.org/10.48550/arXiv.hep-ph/9810242>
- [27] Observation of a new boson at a mass of 125 GeV with the CMS experiment at the LHC, 17 september, 2012
<https://doi.org/10.1016/j.physletb.2012.08.021>
- [28] Abdesslam Arhrib, Rachid Benbrik, Mohamed Chabab and Chuan-Hung Chen Pair production of neutralinos and charginos at the LHC: the role of Higgs bosons exchange, arXiv:1109.0518v3 [hep-ph] 13 Nov 2011
<https://doi.org/10.1103/PhysRevD.84.115012>
- [29] Pavel Fileviez Pérez, Elliot Golias, Alexis D. Plascencia Two-Higgs-Doublet Model and Quark-Lepton Unification, arXiv:2205.02235v1 [hep-ph] 4 May 2022
<https://doi.org/10.1007/JHEP08%282022%29293>
- [30] WILLIAMSON JR, W. Pedestrian Covariant Phase-Space Integration. American Journal of Physics, (1965), 33.12: 987-994.
<https://doi.org/10.1119/1.1971204>
- [31] ALLANACH, Benjamin C., et al. SUSY parameter analysis at TeV and Planck scales. Nuclear Physics, B, (2004), 135, 107
<https://doi.org/10.1016/j.nuclphysbps.2004.09.052>
- [32] K.Desch, J.Kalinowski, G.Moortgat-Pick, M.M.Nojiri and G.Rolesello, JHEP 0402(2004)035 [hep-ph/032069].
<https://doi.org/10.1088/1126-6708/2004/02/035>
- [33] Asmaa .A.A. Production of Neutralino and Higgs Bosons from Electron Positron Collision via Different Propagator, December, 2008
[https://doi.org/10.19138/mtp/\(19\)17-24](https://doi.org/10.19138/mtp/(19)17-24)
- [34] Production of charged and neutral higgs bosons with charginos and neutralinos through different propagators in the MSSM by Hatim Hegab Ali Hegab, arxiv: hep-ph/0608168v2 16 Aug 2006.
<https://doi.org/10.48550/arXiv.hep-ph/0608168>
- [35] Higgs bosons in supersymmetric models - John F. Gunion, SLAC-PUB-3404 Aug 1984.
[https://doi.org/10.1016/0550-3213\(86\)90340-8,10.1016/0550-3213\(93\)90653-7](https://doi.org/10.1016/0550-3213(86)90340-8,10.1016/0550-3213(93)90653-7)
- [36] Zeinab Adel Helmy Ibrahim. Production neutralino and charginos from electron positron annihilation via different propagators, 2021
<https://iiste.org/Journals/index.php/APTA/article/view/56968>
- [37] M.M.Ahmed and Asmaa .A.A. Production of Neutralinos Via H^0 Propagator From Electron – Positron Annihilation, ISSN 2224-719X (Paper) ISSN 2225-0638 (Online) Vol.33, 2014
<https://iiste.org/Journals/index.php/APTA/article/view/14092>
- [38] Gauge cancellation for electroweak processes and the Gervais-Neveu gauge, Y.J. Feng and C.S. Lam, arxiv: hep-ph/9608219v1 2Aug 1996.
<https://doi.org/10.48550/arXiv.hep-ph/9608219>